

Supplemental Material

A Simple Generalized Gradient Approximation for the Non-interacting Kinetic Energy Density Functional

K. Luo,^{1,*} V.V. Karasiev,^{2,†} and S.B. Trickey^{3,‡}

¹*Quantum Theory Project, Department of Physics, University of Florida, Gainesville, FL 32611*

²*Laboratory for Laser Energetics, University of Rochester, Rochester, NY 14623*

³*Quantum Theory Project, Department of Physics and Department of Chemistry, University of Florida, Gainesville, FL 32611*

(Dated: 12 July 2018)

I. LITHIUM PSEUDO-ATOM

As noted in the main paper, the Li pseudo-atom has only a single orbital, thus must have vanishing t_θ , v_θ , and T_θ . This is essentially impossible behavior to reproduce exactly with a GGA KEDF, so it is of interest to see what a particular approximate KEDF does. The crucial test is scf, not post-scf. For perspective, in addition to the BLPS, we considered another local pseudo-potential (LPP), called “mod1”, in its LDA version¹. All the calculations were done with a locally modified version of the APE code².

Fig. 1 summarizes the results. First, one sees that the mod1 LPP is quite similar to the LPP obtained as the s-channel of the Hamann non-local pseudo-potential³ (NLPP) while the BLPS^{4,5} is quite different. However, the Hamann s-channel and BLPS pseudo-densities have a rough qualitative similarity. The mod1 pseudo-density is distinct. All, however, have zero slope at the origin, an important distinction from a cusped density in the context of a GGA KEDF. Second, one also sees that the Hamann calibration of the LKT a parameter is successful in the sense that the scf BLPS LKT and KS pseudo-densities are reasonably close. The LKT-KS comparison is not as good in the mod1 case, a sign of possibly limited transferability. Third, for both BLPS and mod1 LPPs, LKT delivers a non-vanishing v_θ^{LKT} over a substantial range of r and even, in the BLPS case, has $v_\theta^{LKT} < 0$ around $r = 2$ bohr.

Contributions to the LKT non-interacting kinetic energy are listed in Table I for BLPS and mod1. It can be seen that the Pauli energy is non-negligible (around 35%) relative to the VW energy. This non-zero result is certainly a limitation of the GGA KEDF form. However, the total non-interacting kinetic energies from LKT are close to the KS reference values. As must be true for an N -representable approximate KEDF, the exact KS kinetic energy is a lower bound to the LKT value in both cases.

TABLE I. Computed values (Hartree atomic units) of Pauli energy T_θ^{LKT} , von Weizsäcker energy T_W^{LKT} , and total non-interacting kinetic energy from LKT, T_s^{LKT} , together with the reference KS kinetic energy for both BLPS and mod1 LPPs.

	T_θ^{LKT}	T_W^{LKT}	T_s^{LKT}	T_s^{KS}
BLPS	0.018873	0.055018	0.073891	0.069254
mod1	0.025726	0.067051	0.092777	0.091551

II. COMPUTATIONAL TECHNICAL DETAILS - PERIODIC SYSTEMS

Conventional KS calculations were done with ABINIT vers. 8.4.3⁶. The OF-DFT calculations used PROFESS⁷ and/or PROFESS@QUANTUM-ESPRESSO⁸. The KS-DFT calculations used a Fermi-Dirac smearing parameter of 0.01 eV for metals. A $20 \times 20 \times 20$ Monkhorst-Pack⁹ k-point grid was used for all systems. The energy cutoff was 1600 eV in both KS and OF-DFT calculations. We used the “dime=two” option in PROFESS. This option forces both the real-space and Fourier transform integration grid size cardinalities in each crystalline direction to be powers of two (which is optimal in parallel calculations).

For LKT, $a = 1.3$ was used throughout. For the WGC KEDF, we used default parameter values $\alpha = (5 + \sqrt{5})/6$ and $\beta = (5 - \sqrt{5})/6$, as well as γ , 2.7 and 4.2 for metals and semiconductors, respectively, as recommended in Ref. [10]. For the HC KEDF, we used averaged parameters $\lambda = 0.01177$ and $\beta = 0.7143$.

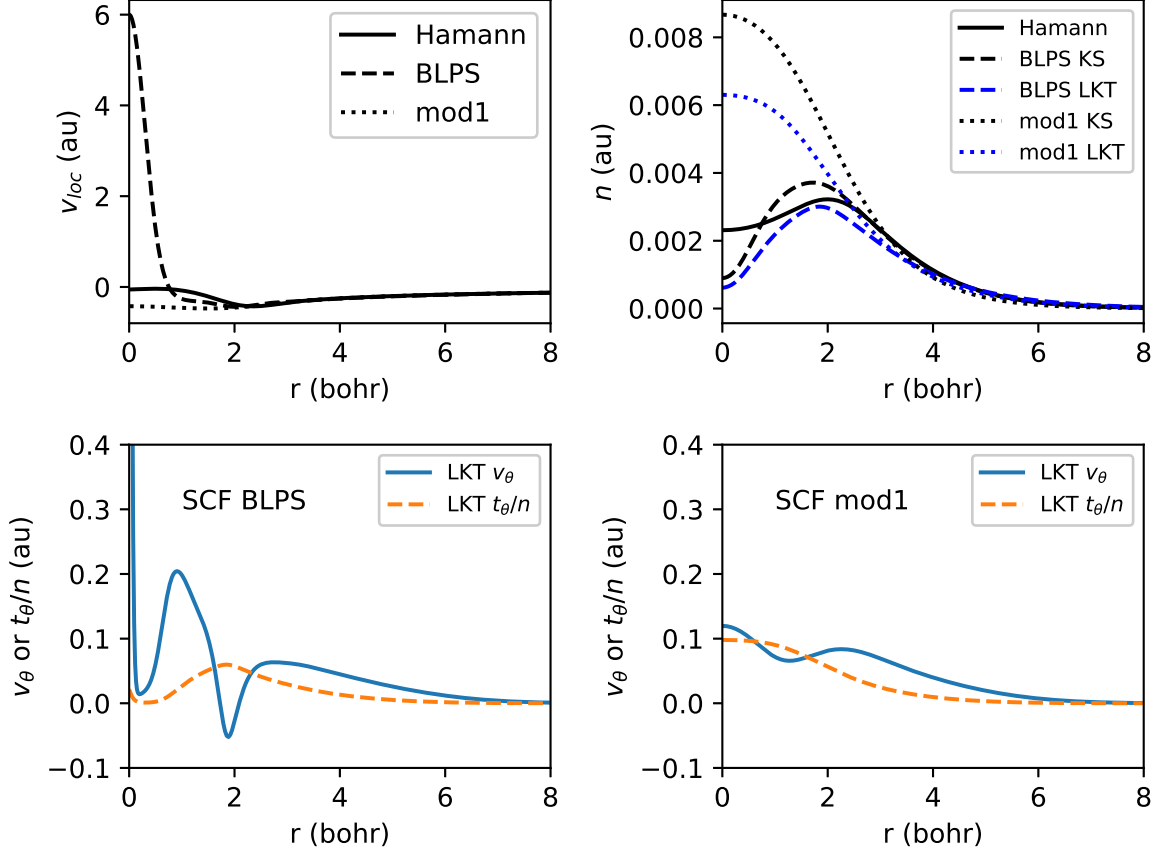


FIG. 1. Top left: BLPS and mod1 LPPs compared with Hamann NLPP s-channel potential; Top right: Li atom KS and LKT pseudo-densities for BLPS and mod1 LPPs along with the Hamann NLPP pseudo-density. Bottom panels: Li pseudo-atom LKT v_θ (solid, blue) and t_θ/n (dashed, orange) for BLPS (left) and mod1 (right) LPPs.

III. DETAILED TABULATION OF RESULTS ON SIMPLE SOLIDS

Detailed results from the validation calculations reported in the main paper are tabulated here. We used the BLPS of LDA type for both KS and OF calculations, including elements Li, Mg, Al, Ga, In, P, As and Sb. Table II gives the results for the metals Li, Mg, and Al for the four KEDFs compared to the KS reference values of V_0 , E_0 , and B_0 . The structures include simple cubic (sc), body-centered cubic (bcc), face-centered cubic (fcc), and hexagonal close packed (hcp). Table III provides the corresponding results for the III-V semiconductors of zinc-blende structure we studied.

With the same data, Fig. 2 shows the differences of V_0 , E_0 (either per atom or per cell), and B_0 between orbital-free calculations and conventional KS reference calculations for various KEDFs. The quantities shown are defined as

$$\Delta Q = Q_{OF} - Q_{KS}, \quad (1)$$

where Q is V_0 , E_0 , or B_0 . The corresponding display for semiconductors is Fig. 3.

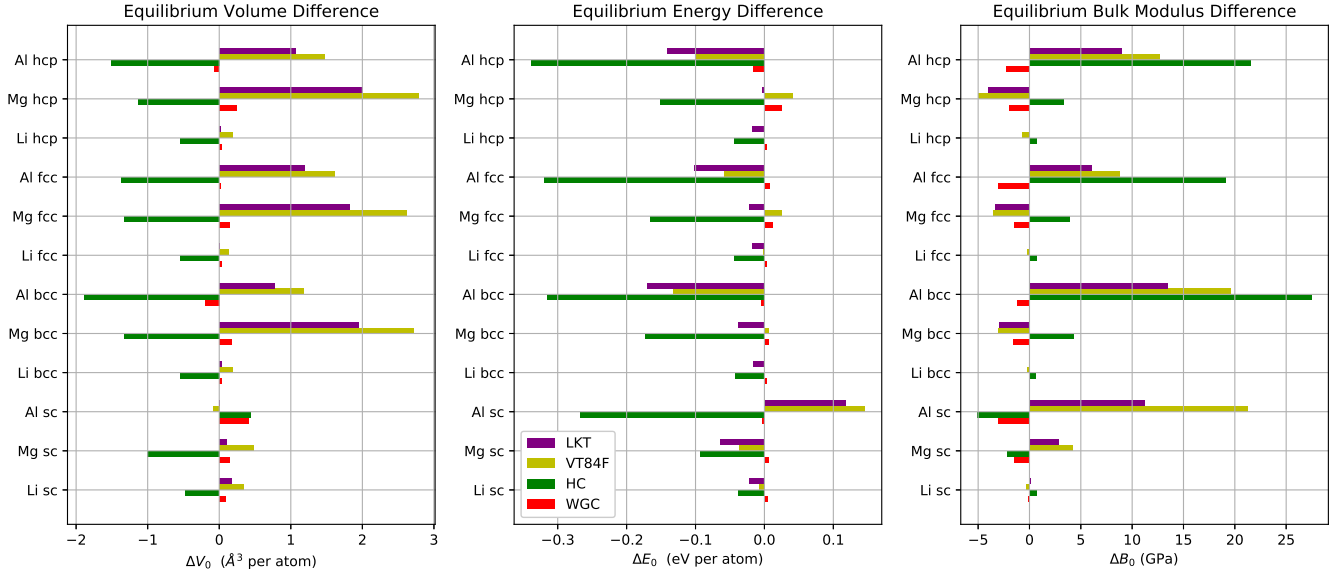


FIG. 2. Differences of equilibrium volume ΔV_0 , energy ΔE_0 , and bulk modulus ΔB_0 between orbital-free calculations with WGC (red), HC (green), VT84F (yellow), LKT (purple), and reference conventional KS calculations for metals. See definitions in Eq. (1).

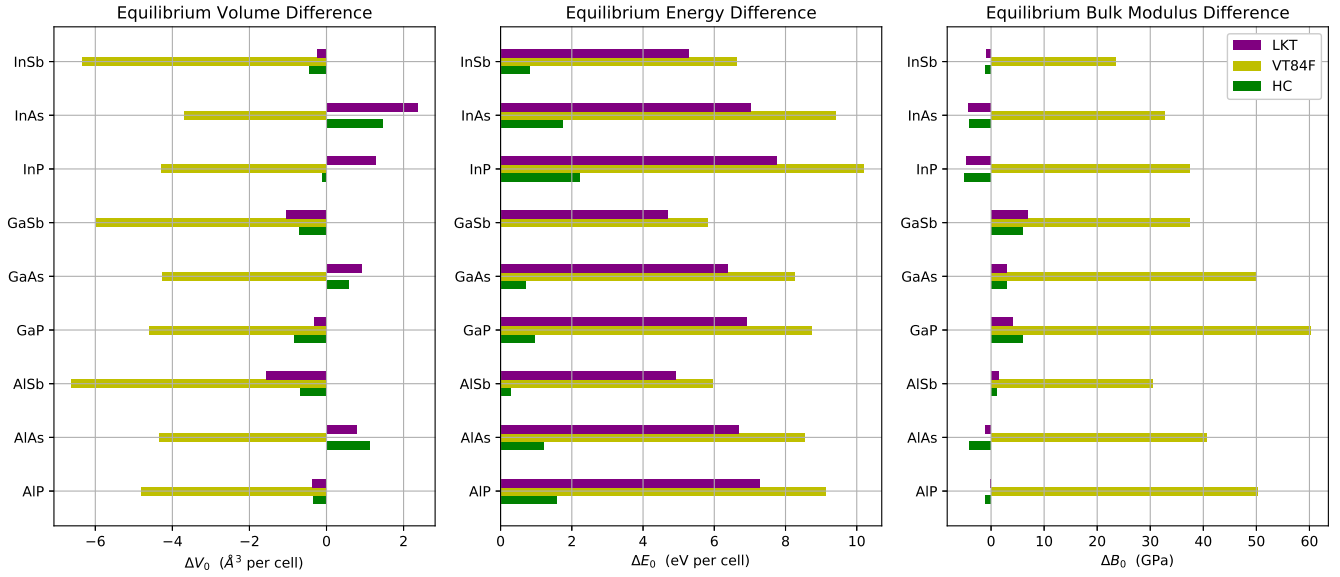


FIG. 3. Differences of equilibrium volume ΔV_0 , energy ΔE_0 and bulk modulus ΔB_0 between orbital-free calculations with HC (green), VT84F (yellow), LKT (purple), and reference conventional KS calculations for semiconductors. Same quantities as in Fig. 2.

TABLE III. Equilibrium volume V_0 ($\text{\AA}^3/\text{cell}$), energy E_0 (eV/cell), and bulk moduli B_0 (GPa) of simple III-V zinc-blende semiconductors. Systems include AlP, AlAs, AlSb, GaP, GaAs, GaSb, InP, InAs, InSb. Conventional KS results are from Ref. [11] except the B_0 for GaP for which we use 88 GPa from our calculation. The HC data are taken from Ref. [11].

	KEDF	AlP	AlAs	AlSb	GaP	GaAs	GaSb	InP	InAs	InSb
V_0	KS	40.637	43.616	56.607	37.646	40.634	52.488	46.040	49.123	62.908
	WGC	-	-	-	-	-	-	-	-	-
	HC	40.290	44.746	55.917	36.795	41.214	51.779	45.930	50.596	62.461
	VT84F	35.827	39.264	49.983	33.027	36.372	46.502	41.755	45.412	56.560
	LKT	40.258	44.417	55.040	37.313	41.546	51.436	47.316	51.492	62.664
E_0	KS	-239.182	-232.908	-206.606	-243.079	-235.799	-209.697	-235.722	-228.537	-202.387
	WGC	-	-	-	-	-	-	-	-	-
	HC	-238.612	-231.702	-206.309	-242.113	-235.086	-209.686	-233.497	-226.775	-201.572
	VT84F	-231.055	-224.355	-200.638	-234.337	-227.528	-203.883	-225.530	-219.116	-195.738
	LKT	-232.910	-226.228	-201.676	-236.168	-229.411	-205.002	-227.971	-221.501	-197.113
B_0	KS	90	80	60	88	75	56	73	65	50
	WGC	-	-	-	-	-	-	-	-	-
	HC	89	76	61	94	78	62	68	61	49
	VT84F	140.3	120.6	90.5	148.3	124.9	93.4	110.4	97.7	73.5
	LKT	89.9	79.0	61.5	92.0	77.9	62.8	68.4	60.7	49.1

* kluo@ufl.edu

† vkarasev@lle.rochester.edu

‡ trickey@qtp.ufl.edu

¹ V.V. Karasiev and S.B. Trickey, Comput. Phys. Commun. **183**, 2519 (2012).

² M.J.T. Oliveira and F. Nogueira, Comput. Phys. Commun. **178**, 524 (2008).

³ D.R. Hamann, M. Schlüter, and C. Chiang, Phys. Rev. Lett. **43**, 1494 (1979) .

⁴ B. Zhou, Y.A. Wang, and E.A. Carter, Phys. Rev. B **69**, 125109 (2004).

⁵ C. Huang, and E.A. Carter, Phys. Chem. Chem. Phys. **10**, 7109 (2008).

⁶ X. Gonze *et. al.*, Computer Phys. Commun. **180**, 2582-2615 (2009).

⁷ L. Hung, C. Huang, I. Shin, G.S. Ho, V.L. Lignères, and E.A. Carter, Comput. Phys. Commun. **181**, 2208 (2010).

⁸ V.V. Karasiev, T. Sjostrom, and S.B. Trickey, Comput. Phys. Commun. **185**, 3240 (2014).

⁹ H.J. Monkhorst and J.D. Pack, Phys. Rev. B **13**, 5188 (1976).

¹⁰ Y.A. Wang, N. Govind and E.A. Carter, Phys. Rev. B **60** 16350 (1999); erratum Phys. Rev. B **64**(E), 089903 (2001).

¹¹ C. Huang, and E.A. Carter, Phys. Rev. B **81**, 045206 (2010).